RSC Advances

PAPER

View Article Online
View Journal | View Issue

Cite this: *RSC Adv.*, 2019, **9**, 23780

Growth of carbon dioxide whiskers†

Avinash Kumar Both and Chin Li Cheung *

Received 18th June 2019
Accepted 24th July 2019

DOI: 10.1039/c9ra04583j

rsc.li/rsc-advances

We report the growth of carbon dioxide (CO_2) whiskers at low temperatures (−70 °C to −65 °C) and moderate pressure (4.4 to 1.0 bar). Their axial growth was assessed by optical video analysis. The identities of these whiskers were confirmed as CO_2 solids by Raman spectroscopy. A vapor–solid growth mechanism was proposed based on the influence of the relative humidity on the growth.

1. Introduction

The study of phase stabilities of molecular solids at high pressures and extreme temperatures is important to understand the nature of chemical bonding, intermolecular interactions, and collective behavior of molecules in condensed phases. For simple molecular systems, it can yield new physical phenomena, ranging from solid–solid phase transitions to complex transformations where the molecular framework itself is profoundly perturbed and new extended materials are attained.[1] This latter case usually occurs when the intermolecular and intramolecular distances converge so that the initial molecular identity is altered, and chemical bonds are reconstructed.[2] Consequently, such new extended materials are usually revealed by their unique growth morphologies, phases, phase transitions and/or covalent bonding motifs. Examples of these systems include the formation of dexamethasone acetate hollow whiskers,[3] metallic deuterium,[4] natural gas clathrate hydrates,[5] new phases of ice,[6] and a new phase of solid iodine.[7]

Carbon dioxide (CO_2) is a chemically stable, linear molecule. It is one of the most important greenhouse gases owing to its ability to absorb and radiate energy in the infrared range and its high abundance in the atmosphere because of the fossil fuel burning activities.[8] To reduce the amount of CO_2 in the atmosphere, researchers have proposed sequestering CO_2 in its solid form by storing it deep under the ground.[9] Although CO_2 is one of the most fundamental chemical species in nature, its solid-phase behavior under high pressures continues to confound the scientific community. Since the discovery of phase III of solid CO_2 by powder X-ray diffraction in 1994,[10] researchers have mapped out a rich CO_2 phase diagram with many additional crystalline phases that range from molecular crystals at lower pressures[11] and in confined nanoslits[12] to extended covalent and ionic phases at high pressures.[13] Experimental characterization of these crystal structures and their solid–solid phase boundaries has often been proven to be a daunting task because the considerable kinetic path-dependence and hysteresis occur in the phase transitions.[14] In addition, the difficulty in acquiring high-quality diffraction data and maintaining sharp pressure gradients within samples that complicate spectroscopic measurements obscure new phase discoveries.[15] As a result, the literature on high pressure solid CO_2 contains numerous contradictory experimental interpretations[16] and further verification studies are indispensable to advance the understanding of CO_2 solids.

Herein, we report our observation of the growth of CO_2 whiskers under low temperature (−70 °C to −65 °C) and moderate pressure (4.4 to 1.0 bar). The growth conditions were attained using a temperature-controlled microscopy pressure stage. The axial growth of these whiskers was evaluated by optical video analysis. A vapor–solid growth mechanism for these whiskers was proposed based on the observed growth process and the dependence of their growth on the relative humidity of the laboratory.

2. Experimental method

(100) Oriented 4″-silicon wafers were purchased from University Wafer (Boston, MA). Solid dry ice and UHP grade CO_2 (Matheson Tri-gas Inc., Montgomeryville, PA) were used as the CO_2 source for the synthesis of CO_2 whiskers.

The growth of CO_2 whiskers was performed inside a Linkam THMS600-PS temperature-controlled microscopy pressure stage (Linkam Scientific Instruments, Tadworth, United Kingdom) and was monitored using an Olympus SZ-STS optical microscope (Olympus Life Science, Center Valley, PA) (see Fig. S1†). Silicon wafers of approximately 1 × 1 cm^2 size were used as substrates for growing the CO_2 whisker materials. The relative humidity (R.H.) of the laboratory was maintained at *ca.* 42% or 65% using a humidifier (Levoit, Anaheim, CA). For each experiment, a silicon wafer was first placed on a quartz crucible located at the temperature-controlled platform inside the stage (see Fig. S1†). After the stage was sealed closed, the stage was first purged and then pressurized with UHP grade CO_2 to 4.4 bar. The sample was cooled down to

University of Nebraska-Lincoln, Lincoln, Nebraska 68588, USA. E-mail: ccheung2@unl.edu

† Electronic supplementary information (ESI) available: Experimental setups, additional images of CO_2 whiskers, CO_2–H_2O phase diagram, and whiskers growth video. See DOI: 10.1039/c9ra04583j

−70 °C at a cooling rate of 5 °C per minute to create a layer of solid CO_2. To initiate the growth of the whisker-like structures, the pressure of the stage was decreased by venting the CO_2 gas through a needle valve of the gas release valve assembly to the laboratory (see Fig. S1†). The pressure of the stage was observed to gradually drop from 4.4 bar to 1.3 bar in the first 30 seconds, but it continued to decrease at a slower rate of *ca.* 0.2 bar per minute for about 1.5 minutes until it reached atmospheric pressure (1.0 bar). During this period, the temperature of the substrate slightly increased from −70 °C to −65 °C. Eventually, the substrate was let warm up naturally to the room temperature. The evolution of the materials growth on the substrate was video recorded. To determine the dependence of whisker growth on R.H. of the laboratory, control experiments were performed either in a laboratory at *ca.* 25–30% R.H. or with the temperature-controlled microscopy pressure stage filled with Type 4A molecular sieves (8–12 mesh size beads, Sigma-Aldrich, Milwaukee, WI) to absorb moisture inside the stage.

Confocal micro-Raman microscopy was performed on a DXR Raman microscope (Thermo Fisher Scientific, LLC, Waltham, MA) equipped with the Linkam temperature-controlled microscopy pressure stage for studying the vibrational signature of CO_2 and water in the as-grown materials (see Fig. S2†). Whisker-like structures were grown using the same conditions as those experiments observed under the Olympus optical microscope. The whiskers and substrates were probed using a 532 nm laser with 5 mW power and a 0.25 μm pinhole aperture.

3. Results and discussion

In our study, we examined the formation of CO_2 whiskers on silicon wafers under moderate pressure (4.4 bar) of CO_2 and at low temperature (−70 °C to −65 °C) inside a temperature-controlled microscopy pressure stage. As the CO_2-pressurized microscopy stage was cooled from room temperature to −70 °C, we observed several sequential phenomena on the silicon substrate: (1) condensation of water vapor as hemispherical droplets, (2) freezing of the water droplets into ice crystals, and (3) condensation of gaseous CO_2 and formation of solid CO_2 (or dry ice) layer over the ice crystals (Fig. 1a–c). Upon the gradual depressurization of the stage from 4.4 bar to 1.0 bar of CO_2 gas, nucleation of particles and growth of whiskers from these particles were observed (Fig. 1d–f and Video: CO_2_-whisker_growth.mp4). The chemical identity of the solid layer over the ice crystals was confirmed to be solid CO_2 by confocal Raman spectroscopy. Typically, the Raman spectrum of CO_2 gas molecules displays two peaks rather than a single peak representing the symmetric stretching of CO_2 in the region of 1250 cm^{-1} to 1450 cm^{-1}. Two peaks are observed because the energy level of the first excited state (ψ_{100}) of the symmetric stretching mode (ν_1) of CO_2 is nearly the same as that of the energy level of the second excited state (ψ_{020}) of the bending vibration ($2\nu_2$) and they have the same symmetry (Σ_g^+). The mixing of these two states into two resulting symmetric states is known as the "Fermi resonance".[17,18] This leads to the re-representation of the symmetric CO_2 vibration mode (ν_1) *via* two experimentally observed Raman peaks at 1285 cm^{-1} and 1388 cm^{-1} in the Raman spectrum and they are commonly referred as the "Fermi diad". This Fermi resonance phenomenon observed in CO_2 is a classic example of strong anharmonic mode–mode coupling. It is not only evident in the gaseous state, but also is found to be pressure-dependent in the solid state.[19] In our experiment, the Raman spectrum of the solid layer showed strong peaks at 1277 cm^{-1} and 1384 cm^{-1}, which matched the locations of the vibration signatures of the Fermi diad in the spectra of our solid CO_2 reference sample and literature data for phase I solid CO_2 (ref. 20) (Fig. 2a). In addition, the intensity ratio of these two

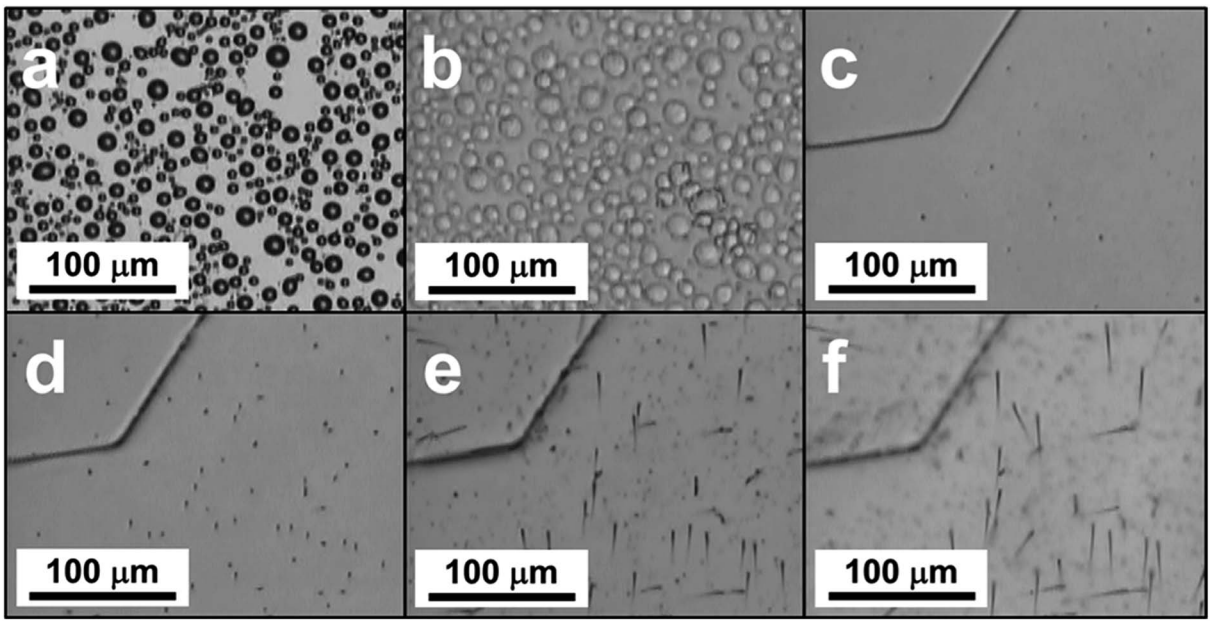

Fig. 1 Chronological illustrations of the CO_2 whiskers growth process: (a) condensation of water vapor into droplets; (b) freezing of water droplets into ice crystals; (c) formation of the solid CO_2 layer over the ice crystals; (d) formation of nuclei on the solid CO_2 layer upon gradual depressurization of the stage; (e) initial growth of CO_2 rod-like structures; (f) growth of CO_2 whiskers.

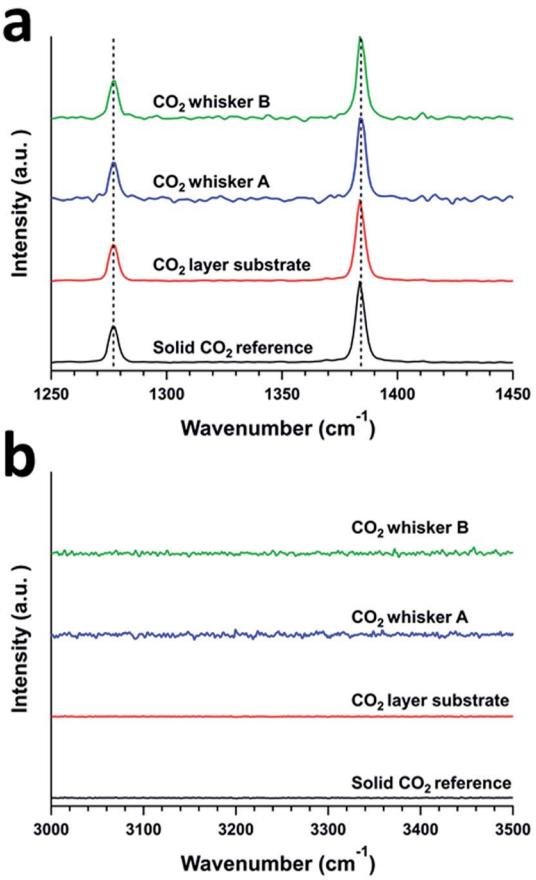

Fig. 2 Confocal Raman spectra of a solid CO_2 reference, a solid CO_2 layer, and CO_2 whiskers A and B. Ranges representing (a) Fermi diad and (b) OH-stretch peaks.

peaks ($I(v_1)/I(2v_2) = 0.39$) also agreed well with those of our solid CO_2 reference. Since no vibration signatures indicating the hydroxyl (OH) stretching mode of water molecules were noticeable in the region of 3000 cm^{-1} to 3500 cm^{-1}, this solid layer did not contain a detectable amount of water and thus was not CO_2 gas clathrate hydrate. Note that upon the formation of the solid layer. As the stage was pressurized with CO_2, gentle but continuous "bubbling" actions observed on this solid layer indicate the phase transition of the solid CO_2 to gaseous CO_2, probably due to the dynamic thermal gradient between the cooling stage and the casing of the stage (Fig. 1c and Video: CO_2_whisker_growth.mp4).

After the microscopy stage was cooled to −70 °C, it was slowly depressurized to initiate the growth of the whisker structures, the pressure of the stage was observed to gradually drop from 4.4 bar to 1.3 bar in the first 30 seconds and it continued to decrease at a rate of *ca.* 0.2 bar per minute for about 1.5 minutes until it reached atmospheric pressure. At the same time, the temperature of the stage was let gradually rise to −65 °C. Nucleation of particles on the solid CO_2 layer started to occur at the start of this process (Fig. 1d). Within 2 minutes, these particles initiated the growth many of small whiskers of lengths of 20 μm to 50 μm and diameters from 1 to 2 μm and they remained at the tip of these whiskers. The lengths of these whiskers grew to 50 μm to 100 μm within 3 minutes (Fig. S3†). Interestingly, the particles at the tips of whiskers were bigger when the experiment was carried out a laboratory at higher R.H. such as 65% *vs.* 42% (Fig. 3). In contrast, when we performed control experiments in a laboratory at low R.H. (such as 25% to 30%), using a microscopy stage filled with type 4A water-absorbing molecular sieves, no whisker-like structures were observed. Therefore, water was involved in the whisker growth process.

Further Raman analysis of the as-grown whiskers revealed that they were composed of CO_2 solids. Similar to the case of the CO_2 solid layer grown on the substrates, the Raman spectra of these whiskers showed strong Fermi diad peaks representing vibrational bands at 1277 cm^{-1} and 1384 cm^{-1} (Fig. 2a). We ruled out that these whiskers were composed of typical CO_2 clathrate hydrates or hydrated CO_2. Though the growth of these whiskers was associated with the high R.H. of the laboratory, no OH vibrational signatures that indicate the presence of water in the whiskers were observed (Fig. 2b). In addition, while the locations of the Fermi diad for the whiskers were similar to those of CO_2 clathrate hydrates or hydrated CO_2 solids, the full width half maxima (FWHM) of these two peaks for the whiskers are *ca.* 4–5 cm^{-1}, which were significantly smaller than the FWHM of similar peaks (*ca.* 8–10 cm^{-1}) for CO_2 clathrate hydrates or hydrated CO_2 solids.[21] Hence, we concluded that the whiskers were composed of mostly molecular CO_2 solid.

The growth mechanism for the whiskers was proposed to be similar to the vapor–liquid–solid mechanism (VLS)[22] or the vapor–solid mechanism (VS)[23] for the growth of semiconductor nanowires and microwires with catalyst seeds. Our observed rapid whisker growth process with distinguished tip features mirrored well with those typically observed for the semiconductor whiskers grown by the VLS or VS processes. The depressurization of the microscopy stage to the laboratory at high relative humidity was found critical to induce the growth process. This suggests that water vapor probably leaked into the stage even though the stage was pressurized above atmospheric pressure. Based on the observed phenomena under the experimental conditions, after the formation of the solid CO_2 layer on the substrate at −70 °C and 4.4 bar of CO_2, the formation mechanisms of CO_2 whiskers was postulated to follow the

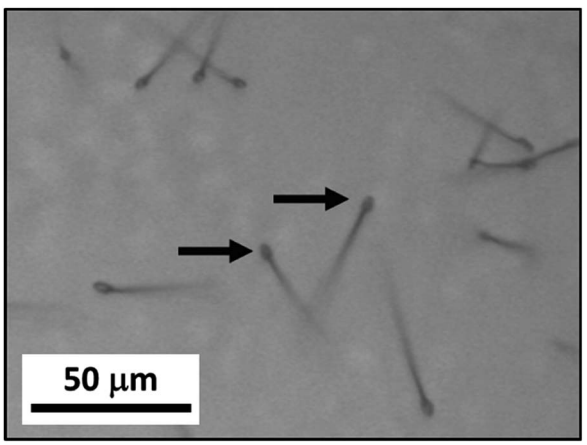

Fig. 3 Optical image of CO_2 whiskers grown when the laboratory R.H. is at 65%. Arrows are indicating the tips of the whiskers.

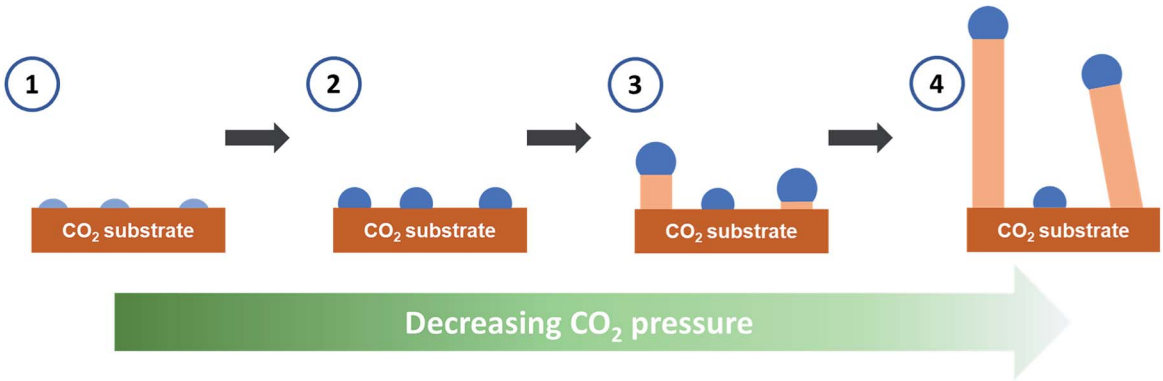

Fig. 4 Schematics for the growth mechanism of the CO_2 whiskers. Light blue: nuclei containing water saturated with CO_2. Blue: particles supersaturated with CO_2. Beige: solid CO_2.

sequential steps shown in Fig. 4. First, as the stage was depressurized from 4.4 bar, water vapor leaked into the microscopy stage through the vent valve assembly and condensed as small nuclei saturated with CO_2 onto the cold surface of the solid CO_2 layer at −70 °C. Second, these condensed nuclei grew into particles supersaturated with CO_2 by continuously absorbing gaseous CO_2 and water vapor available inside the stage. The feasibility for the formation of these complex particles could be inferred from the CO_2–H_2O pressure–temperature (P–T) phase diagram compiled by Genov.[24] In the P–T region of 1 to 4 bar and −70 to −65 °C, a phase boundary existed between solid CO_2 and the coexistence of gaseous CO_2, water ice, and CO_2 hydrate (Fig. S3†), suggesting that the proposed particles of complex compositions could occur under these conditions. Since the stage was continuously depressurized, the solubility of CO_2 in these "seeds" decreased. As the solid CO_2 layer was maintained at about −70 °C, these "seeds" preferentially "precipitated" excess CO_2 on the cold CO_2 layer in the form of whiskers in the third step. Lastly, as more CO_2 dissolved through the tops of these "seeds" to balance the rapid change of their CO_2 concentration, the CO_2 whiskers continued to grow in length with the "seeds" remained at their tops. Note that the whisker growth could be halted by closing the gas release valve during the growth process. This further confirmed that the change in chemical potential of CO_2 in the "seeds" was necessary for the whisker growth.

As aforementioned, water was demonstrated to participate in the CO_2 whiskers growth process, and we postulated its critical role in the nucleation of the CO_2 whiskers. However, similar as for the whiskers, the Raman analysis performed at the whiskers' tips also did not show the OH vibration signatures of water (data not shown). This was possibly due to the weak detection sensitivity to water for the Raman technique[25] and relatively small amount of water in these tips. While the OH stretching vibrations of water are well-known to exhibit strong absorption when examined by the infrared spectroscopy, they have a comparatively much weaker signal in the Raman spectrum of water.[26,27] As the vibrations of the highly polar OH bond does not greatly change its polarizability, the derivative of its polarizability is nearly zero and, hence, the intensity of the OH Raman band is weak. Given that only a miniscule amount of water could be present at the whiskers' tips, it was not unexpected that we might have reached our Raman instrument's detection limit of water at these tips and detect no water signatures. Furthermore, we attempted to perform Raman spectroscopy of the initial nuclei of the tips which might contain higher water content in our postulated mechanism. Nonetheless, as evident in our video data, the whisker growth rate was too fast for us to capture informative Raman spectra using our current instrument.

Our study illustrated the complex behavior of the CO_2–H_2O system and the kinetic-and-composition dependence for the growth of solid CO_2 whiskers. In most CO_2 nucleation models proposed by various theoretical studies,[12,28] CO_2 whisker structures have not been reported. We postulated that it was because these CO_2 whiskers were kinetic products during the phase transitions. We expect that our findings would be of special interests to scientists and engineers working on CO_2 processing research such as CO_2 sequestration. Particularly, understanding the impact of supersaturation of CO_2 in the Earth's and interplanetary environments[29] has lately attracted the attention among the Earth science, space science, and astrophysics communities. For example, many theoretical models have been reported in recent years on understanding the effect of supersaturation of CO_2 in lakes[30,31] and in the formation of caves.[32] In addition, recent studies have reported the formation of solid CO_2 snow[33,34] and CO_2 clathrate hydrate[35] on the surface of Mars. Therefore, our results could help to stimulate renewed understanding of the supersaturation of CO_2 and the phase behavior of water–CO_2 system in environmental and space research.

4. Conclusions

The growth of CO_2 whiskers was demonstrated under moderate pressure (4.4 bar to 1.0 bar) and low temperature (−70 °C to −65 °C). The Fermi diad vibration signatures of CO_2 observed in the confocal Raman spectra of these whisker structures and the absence of OH-stretching vibration signatures indicated that these whiskers were composed of CO_2 with non-detectable water content. Our findings had led to the postulation of a vapor–solid growth mechanism based on the supersaturation

of CO_2 initialed by the condensation of water on the substrates for the formation of whisker-like structures. Additionally, these examples could potentially serve as benchmarks for theoretical models of solid CO_2. Through the re-evaluation of the roles of CO_2 supersaturation, this work could pave a way towards a better understanding of the stochastic nucleation and growth of other one-dimensional molecular solids under phase transition conditions. To resolve more detailed involvement of water in the whisker growth mechanism, other local probe characterization techniques such as *in situ* TEM[36] and confocal infrared spectroscopy,[37] which have higher detection sensitivities for water than Raman spectroscopy, are recommended for future studies.

Conflicts of interest

The authors declare no conflicts of interests.

Acknowledgements

The authors thank the National Science Foundation (Grant #: CHE 1665324) for financial support. We are grateful to Dr Alexander Sinitskii for assistance with the Raman data collection.

Notes and references

1 S. A. Bonev, F. Gygi, T. Ogitsu and G. Galli, *Phys. Rev. Lett.*, 2003, **91**, 065501.
2 R. Bini, *Acc. Chem. Res.*, 2004, **37**, 95–101.
3 F. Mallet, S. Petit, S. Lafont, P. Billot, D. Lemarchand and G. Coquerel, *Cryst. Growth Des.*, 2004, **4**, 965–969.
4 P. M. Celliers, M. Millot, S. Brygoo, R. S. McWilliams, D. E. Fratanduono, J. R. Rygg, A. F. Goncharov, P. Loubeyre, J. H. Eggert, J. L. Peterson, N. B. Meezan, S. Le Pape, G. W. Collins, R. Jeanloz and R. J. Hemley, *Science*, 2018, **361**, 677–682.
5 X. Cao, Y. Huang, W. Li, Z. Zheng, X. Jiang, Y. Su, J. Zhao and C. Liu, *Phys. Chem. Chem. Phys.*, 2015, **18**, 3272–3279.
6 C. Lobban, J. L. Finney and W. F. Kuhs, *Nature*, 1998, **391**, 268–270.
7 Q. Zeng, Z. He, X. San, Y. Ma, F. Tian, T. Cui, B. Liu, G. Zou and H.-k. Mao, *Proc. Natl. Acad. Sci. U. S. A.*, 2008, **105**, 4999–5001.
8 J. Hansen, D. Johnson, A. Lacis, S. Lebedeff, P. Lee, D. Rind and G. Russell, *Science*, 1981, **213**, 957–966.
9 S. Holloway, *Annu. Rev. Energy*, 2001, **26**, 145–166.
10 K. Aoki, H. Yamawaki, M. Sakashita, Y. Gotoh and K. Takemura, *Science*, 1994, **263**, 356–358.
11 J. Li, O. Sode, G. A. Voth and S. Hirata, *Nat. Commun.*, 2013, **4**, 2647.
12 J. Bai, J. S. Francisco and X. C. Zeng, *Proc. Natl. Acad. Sci. U. S. A.*, 2018, **115**, 10263.
13 C.-S. Yoo, *Phys. Chem. Chem. Phys.*, 2013, **15**, 7949–7966.
14 W. Sontising, Y. N. Heit, J. L. McKinley and G. J. O. Beran, *Chem. Sci.*, 2017, **8**, 7374–7382.
15 M. Santoro and F. A. Gorelli, *Chem. Soc. Rev.*, 2006, **35**, 918–931.
16 R. C. Hanson, *J. Phys. Chem.*, 1985, **89**, 4499–4501.
17 P. F. Bernath, *Spectra of Atoms and Molecules*, Oxford University Press, 1995.
18 F. A. Cotton, *Chemical applications of group theory*, Wiley, 1990.
19 O. Sode, M. Keçeli, K. Yagi and S. Hirata, *J. Chem. Phys.*, 2013, **138**, 074501.
20 R. C. Hanson and K. Bachman, *Chem. Phys. Lett.*, 1980, **73**, 338–342.
21 M. Berkesi, K. Hidas, T. Guzmics, J. Dubessy, R. J. Bodnar, C. Szabó, B. Vajna and T. Tsunogae, *J. Raman Spectrosc.*, 2009, **40**, 1461–1463.
22 R. S. Wagner and W. C. Ellis, *Appl. Phys. Lett.*, 1964, **4**, 89–90.
23 A. I. Persson, M. W. Larsson, S. Stenström, B. J. Ohlsson, L. Samuelson and L. R. Wallenberg, *Nat. Mater.*, 2004, **3**, 677–681.
24 G. Y. Genov, PhD thesis, Georg-August-Universität Göttingen, 2005.
25 M. Reichenbächer and J. Popp, *Challenges in Molecular Structure Determination*, Springer Berlin Heidelberg, 2012.
26 S. M. Ali, F. Bonnier, H. Lambkin, K. Flynn, V. McDonagh, C. Healy, T. C. Lee, F. M. Lyng and H. J. Byrne, *Anal. Methods*, 2013, **5**, 2281–2291.
27 L. E. Rodriguez-Saona, M. M. Giusti and M. Shotts, in *Advances in Food Authenticity Testing*, ed. G. Downey, Woodhead Publishing, 1st edn, 2016, ch. 4, pp. 71–116.
28 A. Määttänen, H. Vehkamäki, A. Lauri, S. Merikallio, J. Kauhanen, H. Savijärvi and M. Kulmala, *J. Geophys. Res.*, 2005, **110**, E02002.
29 B. M. Jakosky, *Planet. Space Sci.*, 2019, **175**, 52–59.
30 R. Marcé, B. Obrador, J.-A. Morguí, J. Lluís Riera, P. López and J. Armengol, *Nat. Geosci.*, 2015, **8**, 107.
31 J. K. Lazzarino, R. W. Bachmann, M. V. Hoyer and D. E. Canfield, *Hydrobiologia*, 2009, **627**, 169–180.
32 J. S. Herman, in *Encyclopedia of Caves*, ed. W. B. White, D. C. Culver and T. Pipan, Academic Press, 3rd edn, 2019, ch. 133, pp. 1136–1143.
33 H. E. Chinnery, A. Hagermann, E. Kaufmann and S. R. Lewis, *J. Geophys. Res.: Planets*, 2019, **124**, 337–348.
34 D. L. Glandorf, A. Colaprete, M. A. Tolbert and O. B. Toon, *Icarus*, 2002, **160**, 66–72.
35 A. Dobrovolskis and A. P. Ingersoll, *Icarus*, 1975, **26**, 353–357.
36 S. M. Ghodsi, S. Anand, R. Shahbazian-Yassar, T. Shokuhfar and C. M. Megaridis, *ACS Nano*, 2019, **13**, 4677–4685.
37 P. F. Bernath, *Phys. Chem. Chem. Phys.*, 2002, **4**, 1501–1509.

